2017 IEEE Conference on Control Technology and Applications (CCTA)
August 27-30, 2017. Kohala Coast, Hawai'i, USA

Reduced Order Model Design for Three Way Catalytic Converter Temperature Dynamics

Romit Godi[1], *Student Member, IEEE* and Simona Onori[2], *Senior Member, IEEE*

***Abstract*— This paper presents a reduced order model for three way catalyst (TWC) temperature dynamics developed using Proper Orthogonal Decomposition (POD) and Galerkin projection method. The TWC thermal dynamics are described using a set of coupled, non-linear partial differential equations (PDEs). The Galerkin projection method is applied to the PDE-model to construct a set of ordinary differential equations (ODEs) to describe the dynamics of the system. POD extracts a low dimensional basis functions from a high dimensional data set obtained by numerical simulation of the system. This is achieved by performing singular value decomposition (SVD) on the data set and selecting the basis functions corresponding to the most dominant eigenvalues of the system. Using the POD basis functions along with Galerkin projection leads to a low order ODE system that captures the system dynamics described by the physics based model. The results obtained indicate that the a three state reduced-order model obtained using POD-Galerkin is able to capture the thermal dynamics with satisfactory accuracy. The development of the newly proposed control oriented model for TWC thermal dynamics is carried out using experimental data collected from a TWC running on the Federal Test Protocol (FTP) driving cycle.**

NOMENCLATURE

TWC	Three Way Catalyst	
ODE	Ordinary Differential Equation	
PDE	Partial Differential Equation	
OSC	Oxygen Storage Capacity	$\left[\frac{mol}{m^3}\right]$
λ	Normalized air fuel ratio	
t	Time	$[s]$
z	Spacial coordinate	$[m]$
T_g	Gas temperature	$[K]$
T_{cat}	TWC solid phase temperature	$[K]$
T_{exh}	Exhaust gas temperature	$[K]$
T_{cat_0}	Initial temperature	$[K]$
$\dot{m}_{exh}$	Exhaust gas mass flow rate	$\left[\frac{kg}{s}\right]$
ρ_g	Exhaust gas density	$\left[\frac{kg}{m^3}\right]$
L	TWC length	$[m]$
A_{out}	TWC external surface area	$[m^2]$
V_{cat}	TWC volume	$[m^3]$
$\dot{Q}_{react}$	Heat produced by reactions	$\left[\frac{W}{m^3}\right]$
η	TWC efficiency	

[1]R. Godi is with the Department of Electrical and Computer Engineering, Clemson University, SC, 29634, USA rgodi@clemson.edu
[2]S. Onori is with the Department of Automotive Engineering, Clemson University, Greenville, SC, 29607, USA sonori@clemson.edu

I. INTRODUCTION

Automotive industry has been striving to improve vehicles' efficiency and meet the always more stringent emission standards requiring to governing air pollutants released into the atmosphere [1], [2]. In order to meet the strict emission standards, advances have been made towards both developing advanced engine technologies as well as through powertrain electrification [2]. As the design complexity of automotive engines increases, automakers have been challenged to develop efficient after-treatment systems to control and reduce harmful exhaust gases and particulate matters. Common and harmful exhaust gases under regulation include carbon monoxide (CO), nitrogen oxides (NO_x), and hydrocarbons (HC).

A three way catalyst is the most widespread emission control device used with internal combustion engines in modern vehicles [3]. It reduces simultaneously (NO_x) and oxidize HC and CO with an efficiency close to 99% when the device operates under predefined conditions, namely, engine operation near stoichiometry and sufficiently high temperature [4].

Developing physically-meaningful control oriented models of such devices is the key enabler for improving the device efficiency through the development of robust control and diagnostic strategies. The focus of this paper is the design of a reduced (i.e., control-oriented) model to predict temperature dynamics inside the TWC.

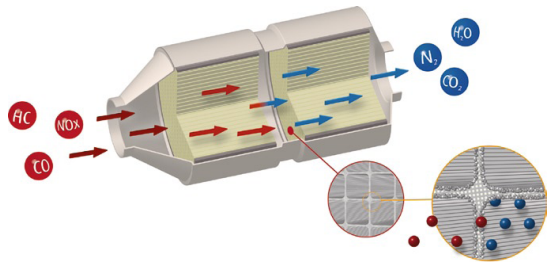

Fig. 1: Schematic view of a TWC (reproduced from [5]).

A three way catalytic converter is redox (reduction-oxidation) reaction-based device in which the harmful pollutants are converted to less toxic emissions.

The efficiency with which the redox reactions occur highly depends on a quantity called air-fuel ratio (AFR). This is the ratio between the mass of air to fuel during combustion process. The AFR is usually denoted in terms of its normalized

value given as:

$$\lambda = \frac{\text{AFR}_{(actual)}}{\text{AFR}_{(stoichiometric)}} = \frac{m_{air}/m_{fuel}}{\text{AFR}_{(stoichiometric)}} \quad (1)$$

where

$$m_{air} = \text{mass of air}$$
$$m_{fuel} = \text{mass of fuel}$$
$$\text{AFR}_{(stoichiometric)} = \begin{cases} 14.7 & \text{for gasoline} \\ 9 & \text{for ethanol} \end{cases} \quad (2)$$

If the AFR is within a narrow region around the stoichiometric value, the chemical reactions occur with higher efficiency, i.e. the success of complete reduction and oxidation reactions is the highest. The efficiency decreases when the AFR falls out of this range. The regions outside of the stoichiometric value are classified as lean and rich conditions. When the AFR is less than the stoichiometric value, the combustion occurs in rich conditions ($\lambda < 1$). In this case the oxygen is utilized during fuel combustion and there isn't sufficient amount left to carry out the oxidation reactions inside the catalyst. When the AFR is greater than the stoichiometric value, the engine operates under lean condition ($\lambda > 1$), i.e there is an excess of oxygen available inside the catalyst, hence the reduction reaction does not occur completely.

The catalytic conversion efficiency also depends on the temperature inside the TWC. Only when the catalyst temperature has reached a threshold level, called light-off temperature, the chemical conversions take place with an efficiency close to 50%. Therefore the catalyst temperature dynamics, plays an imperative role in the control of harmful emissions. The present technology does not allow for such kind of measurement in real-time application. Hence the ability to monitor and predict the catalyst temperature along the flow direction is key to design an efficient exhaust system control strategy.

The common approach to model development to capture the TWC dynamics relies on either physics based or empirical models as in [6], [7], [8] and [9]. The drawback of developing a physics based model is in that the resulting Partial Differential Equation (PDE)-based representation is computationally unfeasible to estimate the real time behavior of the state variable.

When it comes to empirical models, as for example the one proposed in [10], the dependence of the conversion efficiency on the catalyst temperature is neglected, which makes their accuracy a not guaranteed across driving cycles and engine conditions.

This paper proposes a reduced order control-oriented model which not only captures the TWC dynamics efficiently but is also computationally feasible for online implementation. The POD based Galerkin's projection follows a basis function representation of the system obtained by performing singular value decomposition (SVD) on the matrix containing system generated output data. The resulting model simulates the state variables of the TWC system across various driving cycles. *To the best of our knowledge, a rigorous TWC control-oriented model design using formal reduction methods applied to an experimentally validated physics-based system has never been investigated.*

The rest of the paper is organized as follwows: Section II discusses the physics-based PDE model of the TWC. In Section III, the POD-Galerkin's projection method for reduced order modeling (ROM) is presented. In Section IV, the simulation results of the reduced model are presented. Section V gives the conclusion and scope for future work.

II. THREE WAY CATALYST MODEL

The dynamics of the TWC are expressed as a set of coupled nonlinear PDEs [7] describing the temperature profiles of the exhaust gas and the catalyst substrate.

A. Thermal Model

The thermal behavior of the TWC follows a one dimensional approach, and can be described by carrying out energy balance on the exhaust gas and on the solid phase. The gas phase comprises of the exhaust gas flow coming from the engine and flowing into the catalyst and the solid phase is represented by the substrate and the washcoat lumped together [11]. The partial differential equations describing these dynamics are given as follows:

Energy balance of the gas phase

The PDE model describing the energy balance of the gas phase is given by [9]:

$$\rho_g \cdot \epsilon \cdot c_{p_g} \cdot \frac{\partial T_g}{\partial t} = -\frac{\dot{m}_{exh}}{A_{cs}} \cdot c_{p_g} \cdot \frac{\partial T_g}{\partial z} + h \cdot A_{geo} \cdot (T_{cat} - T_g) \quad (3)$$

where $\frac{\partial T_g}{\partial t}$ represents the time dynamics of the gas phase, $\frac{\dot{m}_{exh}}{A_{cs}} c_{p_g} \frac{\partial T_g}{\partial z}$, describes the convective heat transport in the axial dimension and $hA_{geo}(T_{cat} - T_g)$ is the heat exchange between the gas and the solid phase. Considering the gas phase dynamics to be changing rapidly in comparison to the solid phase, we assume the gas temperature T_g to be at steady state. Therefore, the term $\rho_g \epsilon c_{p_g} \frac{\partial T_g}{\partial t}$ is neglected. The simplified equation is:

$$\frac{\dot{m}_{exh}}{A_{cs}} \cdot c_{p_g} \cdot \frac{\partial T_g}{\partial z} = h \cdot A_{geo} \cdot (T_{cat} - T_g) \quad (4)$$

The boundary condition for the above equation is:

$$T_g(z = 0, t) = T_{exh}(t) \quad (5)$$

where the exhaust temperature T_{exh}, measured at the input of the catalyst, is considered to be the initial gas temperature.

Energy balance of the solid phase

The energy balance of the solid phase is described by:

$$\rho_s \cdot (1-\epsilon) \cdot c_s \cdot \frac{\partial T_{cat}}{\partial t} = (1-\epsilon) \cdot \lambda_s \cdot \frac{\partial^2 T_{cat}}{\partial z^2} - h \cdot A_{geo} \cdot (T_{cat} - T_g) + \dot{Q}_{react} - \frac{A_{out}}{V_{cat}} \cdot h_{out} \cdot (T_{cat} - T_{amb}) \tag{6}$$

where the term $\frac{\partial T_{cat}}{\partial t}$, represents the time dynamics of the solid phase, $(1-\epsilon)\lambda_s \frac{\partial^2 T_{cat}}{\partial z^2}$, accounts for the conduction losses in the substrate, $hA_{geo}(T_{cat} - T_g)$ represents the heat exchange between the gas and the solid phase, $\dot{Q}_{react}$ is the heat produced by the exothermic reactions in the washcoat. Finally the term $\frac{A_{out}}{V_{cat}} h_{out}(T_{cat} - T_{amb})$, accounts for the radial losses in the ambient phase. The term $\dot{Q}_{react}$ describes the heat dynamics due to the chemical reactions occurring in the catalyst and is a function of the conversion efficiency. Its dependency on the exhaust mass flow rate is valid under stoichiometric conditions [9]. It can be expressed as follows:

$$\dot{Q}_{react} = K_{react} \cdot \dot{m}_{exh} \cdot \eta(T_{cat}) \tag{7}$$

The contribution of the efficiency term in (7) is significant only above a certain threshold temperature value called $T_{light-off}$ and is generally expressed through a hyperbolic function of the catalyst temperature as [12]:

$$\eta(T_{cat}) = 0.5 \cdot tanh(s(T_{cat} - T_{light-off})) + 0.5 \tag{8}$$

where s is the slope of the efficiency curve. The terms A_{out} and V_{cat} in (6) which represent the TWC external surface area and volume, respectively, are expressed in terms of its diameter by replacing their ration with the term $\frac{4}{D_{cat}}$. The solid phase equation becomes:

$$\rho_s \cdot (1-\epsilon) \cdot c_s \cdot \frac{\partial T_{cat}}{\partial t} = (1-\epsilon) \cdot \lambda_s \cdot \frac{\partial^2 T_{cat}}{\partial z^2} - h \cdot A_{geo} \cdot (T_{cat} - T_g) + \dot{Q}_{react} - \frac{4}{D_{cat}} \cdot h_{out} \cdot (T_{cat} - T_{amb}) \tag{9}$$

The initial condition for (6) is given as:

$$T_{cat}(z, t=0) = T_{cat_0}(z) \tag{10}$$

B. Implementation

The TWC physics-based thermal model is simulated using a the Finite Difference Method (FDM). Although using FDM as a standalone modeling technique does allow for temperature monitoring, the small step size for spacial and time domain results in a large system of ODEs which is not desirable for real time implementation. Decreasing the step size reduces the number of ODEs, but results in large error in comparison to measurement values.

Equations (4) and (9) are discretized with using 40 cell discretization step size over the spacial coordinate and 0.005 seconds as time step. The input signals to the TWC are the exhaust temperature T_{exh}, exhaust gas mass flow rate $\dot{m}_{exh}$, and AFR λ_{pre} measured at the inlet of the catalyst using the sensor layout depicted in Figure 2. The input signals are shown in Figure 3 over the FTP driving cycle.

Parameter	Description
c_{pg}	Specific heat of the exhaust gas $\left[\frac{J}{(kg \cdot K)}\right]$
ϵ	TWC open cross sectional area $[m^2]$
λ_s	TWC solid phase conductivity $\left[\frac{W}{(m \cdot K)}\right]$
$\rho_s c_s$	Volumetric heat capacity of the catalyst $\left[\frac{J}{m^3 \cdot K}\right]$
h	Convective heat transfer coefficient $\left[\frac{W}{m^2 \cdot K}\right]$
h_{out}	Heat transfer coefficient with ambient $\left[\frac{W}{m^2 \cdot K}\right]$
K_{reac}	Scaling factor for $\dot{Q}_{reac}$ term
s	Slope of the TWC efficiency curve function
$T_{light-off}$	Light-off temperature $[K]$
T_{amb}	Ambient temperature $[K]$
A_{cs}	TWC cross sectional area $[m^2]$
A_{geo}	TWC specific geometric area $[m^{-1}]$
D_{cat}	TWC diameter $[m]$
L_{cat}	TWC length $[m]$

TABLE I: List of parameters of the TWC model [9], [13].

The discretized equations are written as:

$$T_g^j = \frac{T_g^{j-1} + \frac{h \cdot A_{geo} \cdot A_{cs} \cdot \Delta z}{\dot{m}_{exh} \cdot c_{p_g}} \cdot T_{cat}^j}{1 + \frac{h \cdot A_{geo} \cdot A_{cs} \cdot \Delta z}{\dot{m}_{exh} \cdot c_{p_g}}} \tag{11a}$$

$$\frac{dT_{cat}^j}{dt} = \frac{\lambda_s}{\rho_s \cdot c_s} \cdot \left(\frac{T_{cat}^{j+1} - 2 \cdot T_{cat}^j + T_{cat}^{j-1}}{\Delta z^2} \right) - \frac{h \cdot A_{geo}}{\rho_s \cdot (1-\epsilon) \cdot c_s} \cdot (T_{cat}^j - T_g^j) + \frac{\dot{Q}_{react}}{\rho_s \cdot (1-\epsilon) \cdot c_s} - \frac{4 \cdot h_{out}}{D_{cat} \cdot \rho_s \cdot (1-\epsilon) \cdot c_s} \cdot (T_{cat}^j - T_{amb}) \tag{11b}$$

Figure 4 shows the solid phase temperature variation simulated using FDM over the FTP driving cycle.

In order to solve the system PDEs, the parameters in it have been previously identified using a Particle Swarm Optimization algorithm [15]. The validated model is found in [9].

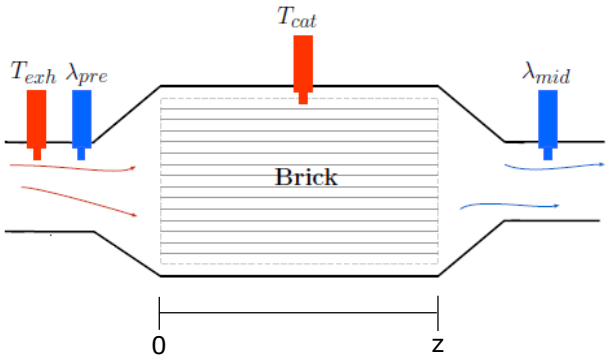

Fig. 2: TWC sensor placement (reproduced from [14]).

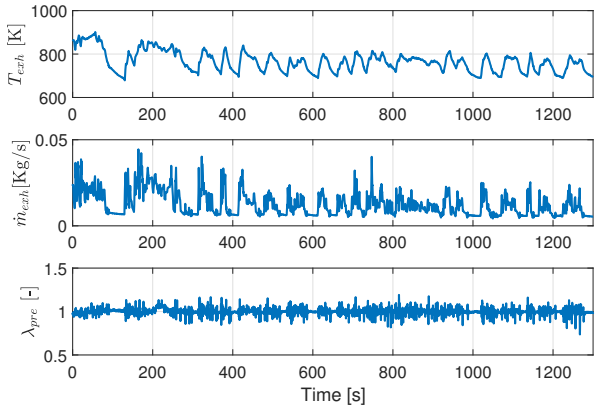

Fig. 3: Inputs to the TWC model over FTP cycle (reproduced from [13]).

III. REDUCED MODEL USING POD-GALERKIN

In this section, we develop a reduced order model of the thermal dynamics of a TWC system using POD-Galerkin projection approach. POD, which is also referred to as Karhunen-Loève decomposition (KLD) or principal component analysis (PCA) [16], is a numerical technique that generates basis functions from system output data [17]. The input to the POD method is a data matrix of the thermal model, in time and spacial domain, computed through simulations over a certain time period and the output is a set of time independent functions that represent the "most energetic" modes of the original system. The basis functions are generated by performing SVD on the data matrix over which the minimum number of modes required to reconstruct the system is selected.

A. Singular Value Decomposition

The data matrix generated from the FDM simulation of Figure 4 is the snapshot matrix S_{snap}, containing values from the system output in time and space domain. SVD is performed on this matrix resulting in the following matrix decomposition,

$$SVD(S_{snap}) = U\Sigma V^T \tag{12}$$

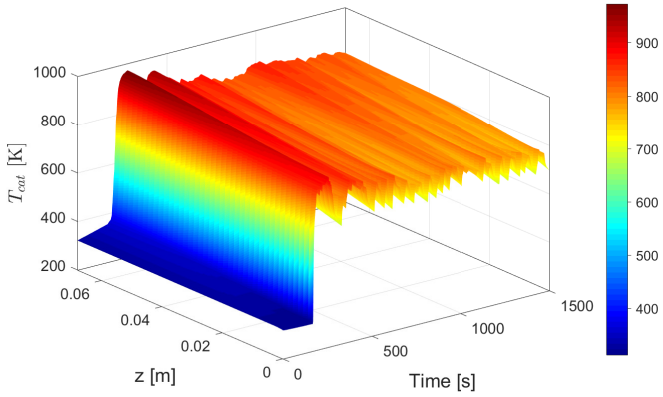

(a)

Fig. 4: Simulation results using FDM over FTP driving cycle for T_{cat}

where

$$U = \begin{bmatrix}\psi_1 & \psi_2 & \dots & \psi_z\end{bmatrix} \in \Re^{zxz}$$
$$V = \begin{bmatrix}v_1 & v_2 & \dots & v_t\end{bmatrix} \in \Re^{txt}$$
$$\Sigma = \begin{bmatrix}\sigma_1 & 0 & \dots & 0 & 0 & \dots & 0\\ 0 & \sigma_2 & & \vdots & & & \\ \vdots & & \ddots & 0 & \vdots & & \vdots \\ 0 & \dots & 0 & \sigma_z & 0 & \dots & 0\end{bmatrix} \in \Re^{zxt} \tag{13}$$

U and V are orthonormal matrices, and Σ is a diagonal matrix containing real positive singular values σ of S_{snap} matrix arranged in decreasing order $\sigma_1 \geq \sigma_2 \geq \dots \geq \sigma_z \geq 0$. The matrix dimension z is the number of discretized cells along the length of the catalyst, which in this case is 40. The dimension t is the number of samples in the driving cycle which in this case is 3,00,000, considering a FTP driving cycle of 1500 seconds sampled at 0.005 second time step. The basis function are contained in the matrix U, and satisfy the properties of orthogonality and orthonormality defined as:

$$\psi_i^T \cdot \psi_j = \begin{cases}1 & \text{if i=j}\\ 0 & \text{if i}\neq\text{j}\end{cases} \tag{14}$$

where $\psi_i(z) =$ space dependent basis functions.

B. Formulating POD basis vectors

The number of modes in the basis function define the order of the reduced model. Since the singular values in the Σ matrix are in decreasing order, the first few values are more dominant in the sense that they capture most of the system dynamics. Hence, a heuristic criterion is applied for selecting the optimal number of basis modes such that the error between the 'actual' dynamics (from the PDE model) and the reduced one is being minimized.

A common approach of selecting the number of modes is by defining an energy criterion as in [18]:

$$O_n = \frac{\sum_{i=1}^{n}\sigma_i^2}{\sum_{i=1}^{N}\sigma_i^2} \tag{15}$$

where

$$\begin{aligned} O_n &= \text{truncation degree} \\ N &= \text{total number of modes} \\ n &= \text{reduced number of modes} \end{aligned} \tag{16}$$

This ratio is used in this work to determine the order of the reduced system model. O_n needs to be close to 1 for the basis functions to reconstruct the approximate solution accurately. This condition is applied to the singular values in the Σ matrix. In order to setup a reduced order model, we set the energy criterion such that the number of modes chosen should capture 99% of the system dynamics. From the plots we conclude that for the temperature dynamics n=3, number of modes satisfy this criteria for FTP the driving cycle.

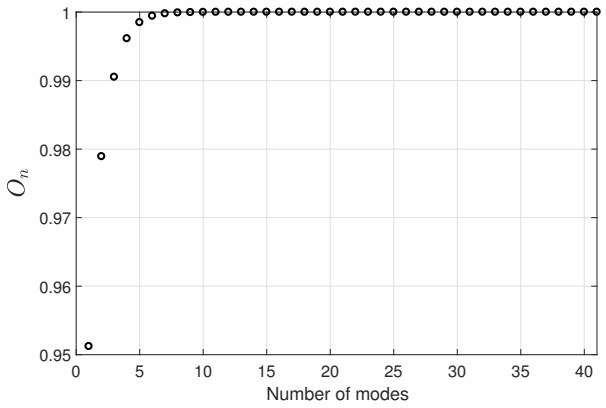

Fig. 5: Truncation degree plot for T_{cat} over FTP driving cycle.

C. Applying Galerkin's projection

The Galerkin's projection approach looks towards developing an approximate solution of a PDE. An exact solution of PDE system is complex due to non-linearity and non-homogeneous boundary conditions. Hence finding an approximate solution with guaranteed accuracy turns out to be a very useful approach. A basis representation of the system PDEs is found by splitting a continuous function (in space and time) into a discrete summation of the two quantities separated. To find the approximate solution, the inner product of the PDE and a weight function is computed over the spacial domain and equated to zero. This ensures that the approximate solution has the least error. The reduced form of the TWC system is derived by applying the Galerkin's projection on the POD basis derived in the previous section. The system variable under consideration in the thermal model is the catalyst temperature. Let us define an approximate solution for T_{cat} as [19]:

$$\begin{aligned} \bar{T}_{cat}(z,t) &= \sum_{i=0}^{n} x_i(t)\,\psi_i(z) \\ &= \psi_n x^T(t) \end{aligned} \tag{17}$$

where

$$\begin{aligned} x^T(t) &= \begin{bmatrix} x_1 & x_2 & \dots & x_t \end{bmatrix} \in \Re^{nxt} \\ \psi(z) &= \begin{bmatrix} \psi_1 \\ \psi_2 \\ \vdots \\ \psi_z \end{bmatrix} \in \Re^{zxn} \end{aligned} \tag{18}$$

$x^T(t)$ are the time dependent fourier coefficients [20] and $\psi_i(z)$ are the space dependent basis functions. The next step is to define the residual function R, as:

$$\begin{aligned} R(\dot{\bar{T}}_{cat}, \bar{T}_{cat}) = \frac{d\bar{T}_{cat}}{dt} - \frac{\lambda_s}{\rho_s \cdot c_s} \cdot \frac{d^2\bar{T}_{cat}}{dz^2} \\ + \frac{h \cdot A_{geo}}{\rho_s \cdot (1-\epsilon) \cdot c_s} \cdot (\bar{T}_{cat} - T_g) \\ - \frac{K_{react} \cdot \dot{m}_{exh} \cdot \left(0.5 \cdot tanh(s(\bar{T}_{cat} - T_{light-off})) + 0.5\right)}{\rho_s \cdot (1-\epsilon) \cdot c_s} \\ + \frac{4 \cdot h_{out}}{D_{cat} \cdot \rho_s \cdot (1-\epsilon) \cdot c_s} \cdot (\bar{T}_{cat} - T_{amb}) \end{aligned} \tag{19}$$

To solve for the approximate solution, we take the inner product of the residual and weight function. The weight function is chosen similar to the basis function as:

$$\left\langle R(\dot{\bar{T}}_{cat}, \bar{T}_{cat}), \psi_j(z) \right\rangle = 0 \tag{20}$$

Substituting the approximate solution of $\bar{T}_{cat}$, we can simplify the above expression as:

$$\left\langle \psi_n \dot{x}^T(t), \psi_j(z) \right\rangle = \left\langle f(\bar{T}_{cat}, u_{cat}, t), \psi_j(z) \right\rangle \tag{21}$$

where,

$$\begin{aligned} f(\bar{T}_{cat}, u_{cat}, t) = \frac{\lambda_s}{\rho_s \cdot c_s} \cdot \left(\frac{d^2\psi_n}{dz^2} \cdot x^T \right) \\ - \frac{h \cdot A_{geo}}{\rho_s \cdot (1-\epsilon) \cdot c_s} \cdot (\psi_n \cdot x^T - T_g) \\ + \frac{K_{react} \cdot \dot{m}_{exh} \cdot \left(0.5 \cdot tanh(s(\psi_n \cdot x^T - T_{light-off})) + 0.5\right)}{\rho_s \cdot (1-\epsilon) \cdot c_s} \\ - \frac{4 \cdot h_{out}}{D_{cat} \cdot \rho_s \cdot (1-\epsilon) \cdot c_s} \cdot (\psi_n \cdot x^T - T_{amb}) \\ u_{cat} = \begin{bmatrix} T_{exh} & \dot{m}_{exh} \end{bmatrix} \end{aligned} \tag{22}$$

contains the non-linear terms of (19). Using the property of orthogonality and orthonormality from (14), and solving for the inner product, the reduced order non-linear model can be written as:

$$\dot{x}^T = \psi^T \cdot f(\bar{T}_{cat}, u_{cat}, t) \tag{23}$$

We can express the above equation in terms of the catalyst temperature by multiplying both sides with ψ_n as follows:

$$\dot{\bar{T}}_{cat} = f(\bar{T}_{cat}, u_{cat}, t) \tag{24}$$

IV. SIMULATION RESULTS

The control-oriented model is compared against the temperature dynamics simulated from the center location of the TWC over a FTP driving cycle. The solid phase temperature T_{cat} simulated by the control oriented model developed using POD-Galerkin using three states is compared to the high

dimensional PDE-based system in Figure 6. The reduced model is able to capture the thermal transients with satisfactory accuracy.

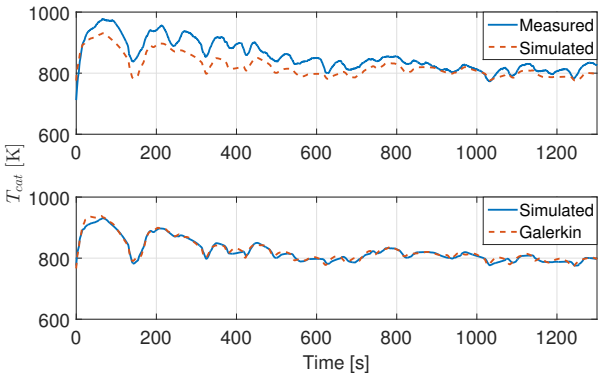

Fig. 6: T_{cat} plot for measured v/s FDM simulated (top) and FDM simulated v/s Galerkin (bottom) values at the center of the catalyst brick.

V. CONCLUSION

In this paper, a control oriented non-linear model is developed for the TWC system with reduced number of modes using the POD-Galerkin projection approach. The basis functions for POD are obtained from a FDM simulated model of the original PDE system. Galerkin projection is then applied to arrive at a control oriented model equation. The truncation degree is plotted to select the order of the control model developed by considering the most dominant modes of the system. From the simulation results, the control-oriented model captures the thermal dynamics with satisfactory accuracy.

REFERENCES

[1] M. Muratori, H. Kheshgi, B. Mignone, L. Clarke, H. McJeon, and J. Edmonds, "Carbon capture and storage across fuels and sectors in energy system transformation pathways," *International Journal of Greenhouse Gas Control*, vol. 57, pp. 34–41, 2016.

[2] EPA. `https://www.epa.gov/clean-air-act-overview/air-pollution-current-and-future-challenges`.

[3] E. Brandt, Y. Wang, and J. Grizzle, "Dynamic modeling of a three-way catalyst for si engine exhaust emission control," *IEEE Transactions on Control Systems Technology*, pp. 767–776, 2000.

[4] A. Faiz, C. S. Weaver, and M. P. Walsh, "Air pollution from motor vehicles: Standards and technologies for controlling emissions," *World Bank Publications*, 1996.

[5] `http://chemistry.umicore.com/Competencies/PassionInChemistry/Automobile/`.

[6] P. Kiwitz, C. Onder, and L. Guzzella, "Control-oriented modeling of a three-way catalytic converter with observation of the relative oxygen level profile," *Journal of Process Control*, vol. 22, no. 6, pp. 984–994, 2012.

[7] T. Shamim, H. Shen, S. Sengupta, S. Son, and A. Adamczyk, "A comprehensive model to predict three-way catalytic converter performance," *Journal of engineering for gas turbines and power*, vol. 124, no. 2, pp. 421–428, 2002.

[8] C. Ngo, D. Koenig, O. Sename, and H. Béchart, "A reduced model of Three Ways Catalyst converter and stored oxygen rate estimation using switched observer," *12th biannual European Control Conference*, 2013.

[9] S. Sabatini, I. Kil, J. Dekar, T. Hamilton, J. Wuttke, M. A. Smith, M. A. Hoffman, and S. Onori, "A New Semi-Empirical Temperature Model for the Three Way Catalytic Converter," *IFAC Workshop on Engine and Powertrain Control, Simulation and Modeling E-COSM*, vol. 48, no. 15, pp. 434–440, 2015.

[10] M. Soumelidis, R. Stobart, and R. Jackson, "A Nonlinear Dynamic Model for Three-Way Catalyst Control and Diagnosis," *SAE Technical Paper Series*, 2014.

[11] R. M. Heck, R. J. Farrauto, and S. T. Gulati, *Catalytic air pollution control: commercial technology*. John Wiley & Sons, 2009.

[12] S. B. Kang, S. J. Han, I. C. Nam, B. K. Cho, C. H. Kim, and S. H. Oh, "Detailed reaction kinetics for double-layered Pd/Rh bimetallic TWC monolith catalyst," *Chemical Engineering Journal*, 2014.

[13] S. Sabatini, S. Gelmini, M. A. Hoffman, and S. Onori, "Design and experimental validation of a physics-based oxygen storage - thermal model for three way catalyst including aging," in *Control Engineering Practice*, 2017.

[14] S. Gelmini, S. Sabatini, M. A. Hoffman, and S. Onori, "Development and experimental validation of a dual extended kalman filter for three way catalytic converter," in *American Control Conference*, 2017.

[15] S. Ebbesen, P. Kiwitz, and L. Guzzella, "A generic particle swarm optimization Matlab function," *Proceedings of the American Control Conference*, 2012.

[16] R. Pinnau, "Model reduction via proper orthogonal decomposition," vol. 13, pp. 95–109, 2008.

[17] W. H. Schilders, H. A. van der Vorst, and J. E. Rommes, *Model Order Reduction: Theory, Research Aspects and Applications*. Springer, 2008.

[18] A. Marquez, J. Oviedo, and D. Odloak, "Model reduction using proper orthogonal decomposition and predictive control of distributed reactor system," *Journal of Control Science and Engineering*, 2013.

[19] S. Oh and J. Cavendish, "Transients of monolithic catalytic converters: Response to step changes in feedstream temperature as related to controlling automobile emissions," *Industrial & Engineering Chemistry Product Research and Development*, no. 21, pp. 29–37, 1982.

[20] D. Luchtenburg, B. Noack, and M. Schlegel, "An introduction to the POD Galerkin method for fluid flows with analytical examples and MATLAB source codes," in *Technical Report*, Berlin Institute of Technology, 2009.